

SANDIA REPORT

SAND2024-05484

Printed May 2024



Sandia
National
Laboratories

Heat Transfer Through a Passive Fire Protective Board from an Impinging Hydrogen Flame

Gabriela Bran Anleu, Christina Felipe, Myra Blaylock, Chris LaFleur

Prepared by
Sandia National Laboratories
Albuquerque, New Mexico
87185 and Livermore,
California 94550

Issued by Sandia National Laboratories, operated for the United States Department of Energy by National Technology & Engineering Solutions of Sandia, LLC.

NOTICE: This report was prepared as an account of work sponsored by an agency of the United States Government. Neither the United States Government, nor any agency thereof, nor any of their employees, nor any of their contractors, subcontractors, or their employees, make any warranty, express or implied, or assume any legal liability or responsibility for the accuracy, completeness, or usefulness of any information, apparatus, product, or process disclosed, or represent that its use would not infringe privately owned rights. Reference herein to any specific commercial product, process, or service by trade name, trademark, manufacturer, or otherwise, does not necessarily constitute or imply its endorsement, recommendation, or favoring by the United States Government, any agency thereof, or any of their contractors or subcontractors. The views and opinions expressed herein do not necessarily state or reflect those of the United States Government, any agency thereof, or any of their contractors.

Printed in the United States of America. This report has been reproduced directly from the best available copy.

Available to DOE and DOE contractors from

U.S. Department of Energy
Office of Scientific and Technical Information
P.O. Box 62
Oak Ridge, TN 37831

Telephone: (865) 576-8401
Facsimile: (865) 576-5728
E-Mail: reports@osti.gov
Online ordering: <http://www.osti.gov/scitech>

Available to the public from

U.S. Department of Commerce
National Technical Information Service
5301 Shawnee Rd
Alexandria, VA 22312

Telephone: (800) 553-6847
Facsimile: (703) 605-6900
E-Mail: orders@ntis.gov
Online order: <https://classic.ntis.gov/help/order-methods/>



ABSTRACT

This report documents analysis to determine whether a hydrogen jet flame impinging on a tunnel ceiling structure could result in permanent damage to the Callahan tunnel in Boston, Massachusetts. This tunnel ceiling structure consists of a passive fire protective board supported by stainless steel hangers anchored to the tunnel ceiling with epoxy. Three types of fire protective boards were considered to determine whether heat from the flame could reach the stainless-steel hangers and the epoxy and cause the ceiling structure to collapse. Heat transfer analyses performed showed that the temperature remains constant where the steel hangers are attached to the passive fire protective board. According to these results, the passive fire protective board should provide adequate protection to the tunnel structure in this release scenario. Tunnel structures with similar suspended fire-resistant liner board materials should protect the integrity of the structure against the extremely low probability of an impinging hydrogen jet flame.

ACKNOWLEDGEMENTS

This material is based upon work supported by the U.S. Department of Energy's Office of Energy Efficiency and Renewable Energy (EERE) under the Hydrogen and Fuel Cell Technologies Office (HFTO) Safety Codes and Standards sub-program, under the direction of Laura Hill. The authors also wish to thank Justin Slack and John Czach from the Massachusetts Department of Transportation (MassDOT) and Charles Myers from the Massachusetts Hydrogen Coalition for their help in providing tunnel information and feedback on the analysis. The authors gratefully acknowledge Melissa Louie, Dusty Brooks, Ben Schroeder, Marina Miletic, and Brian Ehrhart from Sandia National Laboratories for their review of this work.

CONTENTS

Abstract	3
Acknowledgements	4
Contents	5
List of Figures	5
List of Tables.....	6
Acronyms and Terms.....	8
1. Introduction.....	9
1.1. Fire Scenario	9
1.2. Previous CFD Simulations of Hydrogen Flame Impingement	9
1.3. Tunnel Structure	11
1.3.1. Material Properties.....	11
2. Numerical Simulations.....	15
2.1. Numerical Domain	15
2.2. Mathematical Model.....	17
2.2.1. Energy Conservation Equation	17
2.2.2. Initial and Boundary Conditions	17
2.3. Mesh Refinement.....	19
3. Results.....	23
3.1. PROMATECT-H with Constant Material Properties.....	23
3.2. PROMATECT-H with Variable Material Properties.....	25
3.3. PROMATECT-L500 with Variable Material Properties	27
3.4. Temperature at Adhesive Location.....	29
4. Summary and Conclusions	31
References.....	34
Distribution	35

LIST OF FIGURES

Figure 1: (a) Blowdown of a 125L (0.125 m ³) high pressure hydrogen tank showing mass flow rate on the left blue axis and the hydrogen visible flame length [4] on the right red axis, and (b) the velocity of the blowdown for the tank with a 2.25 mm TPRD orifice [4]. (c) The total hydrogen mass released as a function of time for a 5.25 cm TPRD orifice and constant mass flow rate, showing when 5 kg are released.	10
Figure 2. Cross-sectional view of the Callahan tunnel [6]. The 2-inch (5.08-cm) layer of Promat is supported by steel hangers [6, 7]. The 2-inch (5.08-cm) layer of Promat would encounter the hydrogen flame prior to the steel hangers since it comprises the bottom layer of the structure. .	11
Figure 3. Temperature dependent a) density, b) thermal conductivity, and c) specific heat and mass loss for PROMATECT-H (left) and PROMATECT-L500 (right) [5].	13
Figure 4: Isometric view of fire protective board used in heat transfer model. Fire protective board has a length of 600 inches (1524 cm), a width of 280 inches (713 cm), and a thickness of 2 inch (5.1 cm). All surfaces are assumed to be insulated except the bottom surface where convection and radiation are prescribed. Temperature T1-T11 are located every 0.2 inch (0.5 cm) across the thickness of the Promat. (Figure not to scale).....	16

Figure 5. Boundary conditions applied on bottom surface of tunnel ceiling structure: (a) temperature map from [4], (b) the radial temperature, (c) convective heat transfer coefficient, and (d) irradiation plotted with respect to the r-axis measuring radial length from the center of the flame impingement on the bottom surface.....	18
Figure 6. Temperature at the bottom surface (top-left), at 0.5 cm (top-right), 1.0 cm (bottom-left), and 1.5 cm (bottom-right) from the bottom surface for intervals 2 to 12. When the thickness is divided into 10 intervals or more, the mesh is sufficiently fine.....	20
Figure 7. The final mesh used for the heat transfer analysis discretized the thickness of the Promat by 12 intervals. The mesh contains 13,039,344 elements (14,155,050 nodes).	20
Figure 8. Bottom view of the biased mesh (left) and close-up bottom view of the biased mesh (right). A bias was applied within a 3.3 meters radius on the bottom surface. The element size on the outer radius was applied to the edges of the slab to preserve symmetry where possible. .	21
Figure 9. Isometric view of biased mesh used in Callahan tunnel simulations.....	21
Figure 10. Heat transfer simulation results produced by the fine mesh and biased mesh were compared to ensure that the biased mesh produced sufficient accuracy. Plot shows the bottom surface temperature of PROMATECT-H over the span of 5 minutes.	22
Figure 11. Temperature distribution across a 2-inch thick PROMATECT-L500 slab using variable material properties at different time steps. From top to bottom: 0, 0.83 minutes, 1.3 minutes, and 5 minutes. Maximum and minimum values are specified for each time step.	24
Figure 12. Transient temperature distributions at every 0.2 inch a) from the bottom surface ($y=0$) to the top surface ($y=2$ inches) and b) from $y=1$ inch to the top surface ($y=2$ inches) are shown for a PROMATECT-H slab with constant properties. Note that the scale of the y -axis on the figures is different.	25
Figure 13. From top to bottom; temperature profile at center ($x=z=0$) of PROMATECT-H with variable material properties of thickness 2 inches (5 cm) at 0, 0.83 minutes, 1.3 minutes, and 5 minutes.	25
Figure 14. Temperature profile across the thickness for a Promat slab with variable properties of PROMATECT-H.	26
Figure 15. Temperature profiles across the thickness of the PROMATECT-H slab in the Callahan tunnel at different time steps show that at $y = 2$ inches the temperature is still ambient which corresponds to the location where the two slabs are attached.	27
Figure 16. Temperature distribution across a 2-inch thick PROMATECT-L500 slab using variable material properties at different time steps. From top to bottom: 0, 0.83 minutes, 1.3 minutes, and 5 minutes. Maximum and minimum values are specified for each time step.	27
Figure 17. Temperature profile across the thickness for a Promat slab with variable properties of PROMATECT-L500.	28
Figure 18. Temperature profiles across the thickness of the PROMATECT-L slab in the Callahan tunnel at different time steps show that at $y = 2$ inches the temperature is still ambient which corresponds to the location where the two slabs are attached.	28
Figure 19. For each material, temperature profile with respect to time at the location of the adhesive which bonds two slabs of Promat.....	29

LIST OF TABLES

Table 1. Constant material properties used for first heat transfer analysis.....	12
Table 2. Material properties and mesh used for each heat transfer analysis	19
Table 3. Summary of temperatures of the Callahan tunnel at $t = 0.83$ minutes, 1.3 minutes, and 5 minutes.	33

This page left blank

ACRONYMS AND TERMS

Acronym/Term	Definition
AHJ	authority having jurisdiction
CFD	computational fluid dynamics
FCEV	fuel cell electric vehicle
FEM	finite element method
PDE	partial differential equation
TPRD	thermally-activated pressure release device

1. INTRODUCTION

Hydrogen fuel cell electrical vehicles (FCEVs) can help decrease greenhouse emissions coming from the transportation sector as an alternative to gasoline vehicles [1]. The safety implications of hydrogen should be considered for use cases where this fuel type would have different responses than typical gasoline or diesel fuels, such as in the case a hydrogen FCEV involved in a fire inside a tunnel. Chapter 7 of the National Fire Protection Association Standard for Road Tunnels, Bridges, and Other Limited Access Highways (NFPA 502) provides recommendations to ensure tunnel safety to the authority having jurisdiction (AHJ) [2], which is responsible for enforcing the requirements of a code or standard. Annex G of NFPA 502 explains that these requirements do not consider alternative fuels, such as hydrogen. Instead, the requirements were developed for gasoline, ethanol, and diesel fuels. The differences between a hydrogen fire and gasoline fire are listed in [1], but the most important ones are that hydrogen releases from a light duty hydrogen FCEV last no more than 5 minutes, but the temperature of a hydrogen fire is significantly higher than the temperature of a gasoline fire. NFPA 502 entrusted the responsibility to the AHJ of deciding to allow vehicles that use alternative fuels to utilize their tunnels and establishing mitigation once they are approved. As stated in Chapter 4 and 7 of NFPA 502, the AHJ should perform an engineering analysis when the consequences of a fire are in doubt. This engineering analysis should also be used to establish mitigations for those consequences.

Some AHJs were interested in learning about the severity of a specific low-probability high-consequence scenario involving a hydrogen FCEV for a tunnel similar to the Callahan tunnel structure in Boston, Massachusetts. This tunnel comprised of a fire protective board supported by stainless-steel hangers anchored to the ceiling of the tunnel with epoxy. Three types of fire protective boards were considered to determine if heat from the flame could reach the stainless-steel hangers and the epoxy and cause the structure to collapse. The temperature of the tunnel ceiling structure was modeled using the thermal module Aria from the Sandia-developed Sierra suite [3]. The boundary conditions used in this study were obtained from a computational fluid dynamics (CFD) analysis performed by the authors in [4] where they modeled a hydrogen jet flame impinging on a flat ceiling surface with and without ventilation. Only the no ventilation case was used in this study because it is the worst-case scenario. A mesh refinement study was performed to ensure that the temperatures obtained across the structure are independent of the mesh size.

1.1. Fire Scenario

The low-probability high-consequence scenario of interest consists of a gasoline vehicle colliding with a hydrogen FCEV. A fire caused by a gasoline leak triggers the high-pressure hydrogen tank thermally-activated pressure relief device (TPRD) to release the 5 kg of hydrogen from an orifice with a diameter of 2.25 mm in approximately 5 minutes as shown in Figure 1a (blue line). The combination of high pressure in the tank and the small TPRD orifice results in a choked flow with an average velocity of 700 m/s (see Figure 1b). Hydrogen ignites due to the heat from the gasoline fire resulting in a hydrogen jet flame [4]. The hydrogen jet flame impinges on the ceiling of the tunnel for about 1.3 minutes as shown in Figure 1a (red line).

1.2. Previous CFD Simulations of Hydrogen Flame Impingement

The authors in [4] performed a CFD simulation of a hydrogen flame impinging on a flat surface located 16 ft from the tunnel ground. The heat flux from the CFD simulations serve as boundary conditions in the heat transfer simulations they performed on selected ceiling structures. To reduce the computational expense of the CFD simulations and reduce the Mach number at the orifice, the

authors assumed a 5.25 cm TPRD orifice diameter (instead of 2.25 mm) and a constant velocity of 700 m/s (instead of the varying velocity shown in Figure 1b). Due to the high computational cost, the CFD simulations were run up to 3.3 seconds of release. The authors in [4] used the heat flux at 3.3 seconds as the constant boundary condition at the ceiling structure surface in their heat transfer simulations. The simulations were run for 5 minutes, which represent the time a full 5-kg hydrogen tank takes to completely empty. Using a constant heat flux for duration of the release means that the mass flow rate at 3.3 seconds was also constant for the duration of the release. In other words, the blowdown shown in Figure 1a was not included in their heat transfer simulations. With this assumption, a total of 30 kg of hydrogen was released in 5 minutes instead of 5 kg, and it took only 0.83 minutes to release 5 kg of hydrogen as shown in Figure 1c.

In this work, the CFD results at 3.3 seconds are used as boundary conditions at the bottom surface of the ceiling structure. Temperatures at 0.83 minutes and 1.3 minutes are presented in this report, but results for a duration of 5 minutes are also noted. The heat transfer simulations do not model the decomposition of the fire protective board. However, density, thermal conductivity, and specific heat used in this study are from measurements done on decomposing specimens, so heat transfer calculations are affected by the changing thermal properties due to temperature increase and mass loss. Mass loss experimental measurements found in [5] was used to determine if mass loss occurs during the heating process (see Section 1.3.1 for more details).

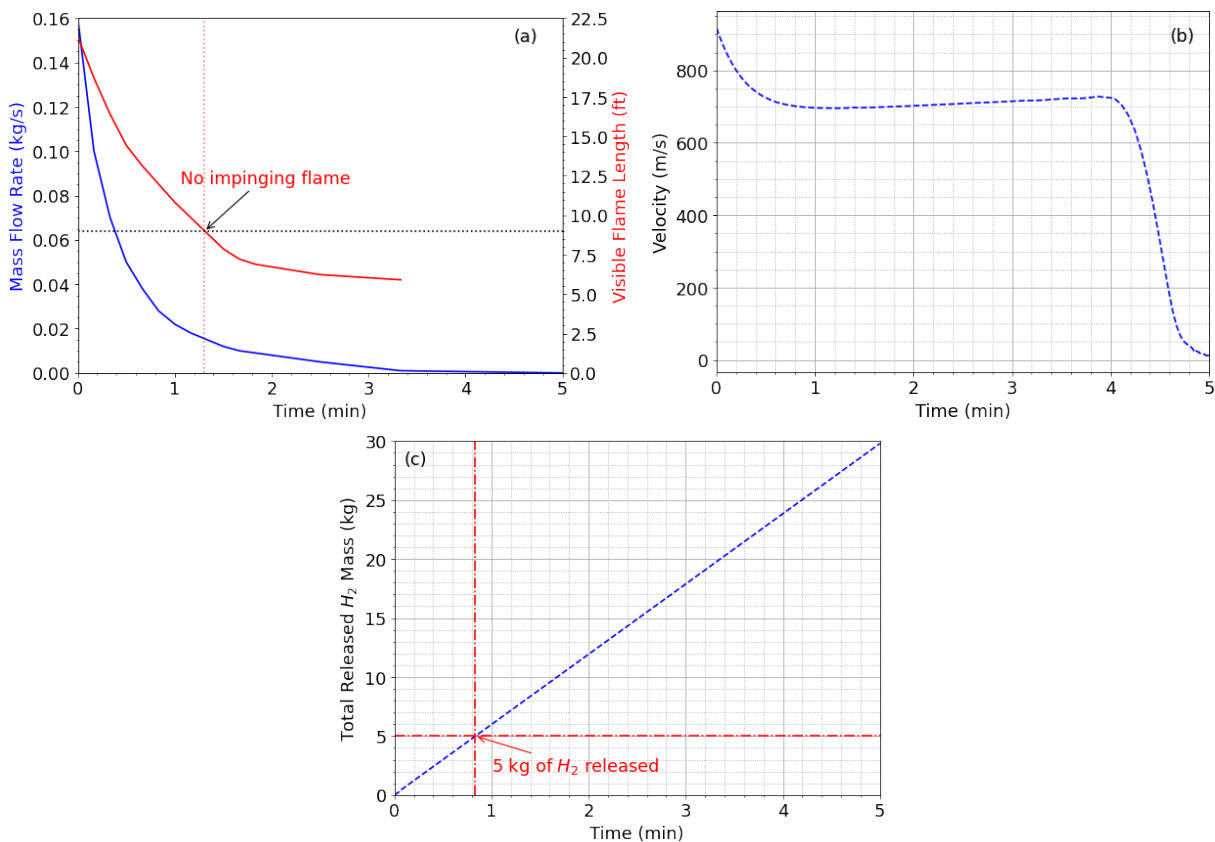


Figure 1: (a) Blowdown of a 125L (0.125 m³) high pressure hydrogen tank showing mass flow rate on the left blue axis and the hydrogen visible flame length [4] on the right red axis, and (b) the velocity of the blowdown for the tank with a 2.25 mm TPRD orifice [4]. (c) The total hydrogen mass released as a function of time for a 5.25 cm TPRD orifice and constant mass flow rate, showing when 5 kg are released.

1.3. Tunnel Structure

The Callahan tunnel ceiling structure consists of passive fire protective boards supported by stainless-steel hangers anchored to the tunnel ceiling with epoxy (see Figure 2). The passive fire protective board is 14 feet (4.3 m) from the tunnel roads. Figure 2 also shows a more detailed schematic of how the fire protective board is attached to the stainless-steel hangers. Two 1-inch (2.54-cm) fire protective layers are bound together with an unknown material, and the exposed surfaces are coated with a porcelain enamel. As shown in Figure 2, each hanger is attached to the top of two 2-inch (5.08 cm) slabs with bolts and washers. Structural silicone closes the 1/2-inch (1.27-cm) gap between the two slabs.

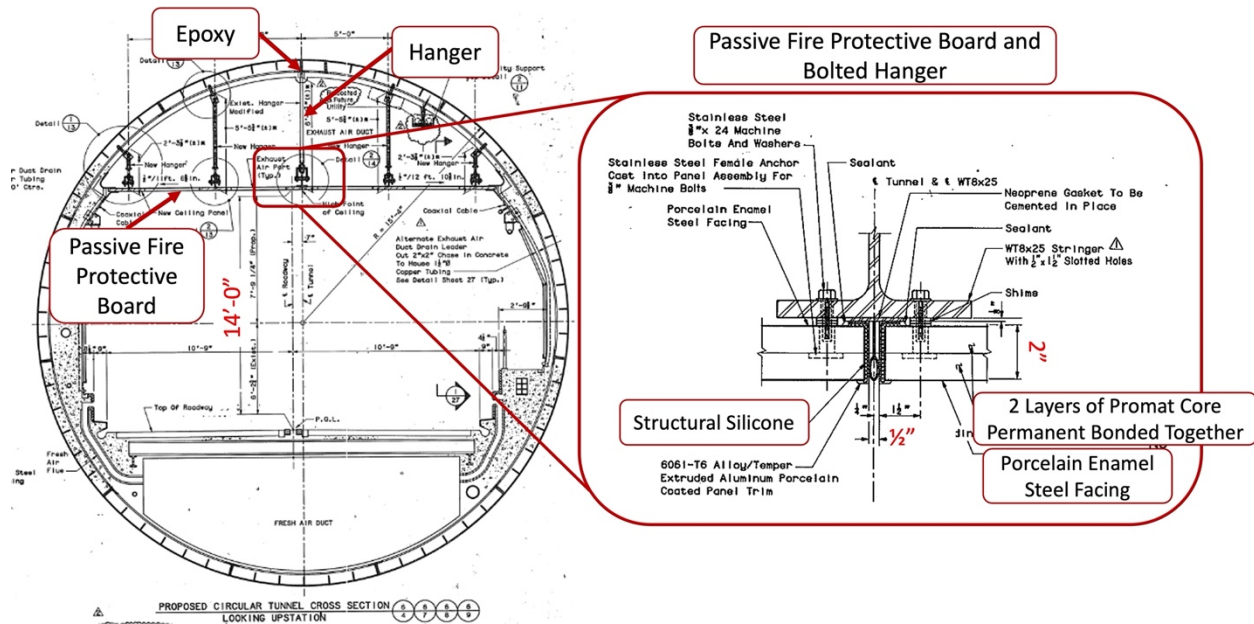


Figure 2. Cross-sectional view of the Callahan tunnel [6]. The 2-inch (5.08-cm) layer of Promat is supported by steel hangers [6, 7]. The 2-inch (5.08-cm) layer of Promat would encounter the hydrogen flame prior to the steel hangers since it comprises the bottom layer of the structure.

1.3.1. Material Properties

Figure 2 specifies that the fire protective slab is made from a material called Promat, but it does not specify which type of Promat material was used. The vendor, Promat Inc., offers six types of passive fire protection boards for tunnels [8]:

1. PROMATECT-H,
2. PROMATECT-H RWSHCM,
3. PROMATECT-L500,
4. PROMATECT-T,
5. DURASTEEL, and
6. PROMATECT-TF-X.

Promat also offers an adhesive, PROMACOL-S, for tunnel applications. PROMACOL-S is used with PROMATECT-H and PROMATECT-L500 boards [8]. It is likely that the fire protective boards consist of PROMATECT-H or PROMATECT-L500 and that the adhesive used to bond the two Promat layers is PROMACOL-S. Three cases were defined based on these assumptions, using either

constant or temperature-dependent thermal properties for PROMATECT-H and temperature-dependent thermal properties for PROMATECT-L500.

The first heat transfer simulation assumed conservative constant property values for the PROMATECT-H material [9]. Since the emissivity of PROMATECT-H was not publicly available, the emissivity of PROMALITE was used instead [10]. Table 1 lists the constant thermal properties used in the first heat transfer analysis.

Table 1. Constant material properties used for first heat transfer analysis

Material	Material Property	Value
PROMATECT-H	Density (ρ)	$870 \frac{kg}{m^3}$
PROMATECT-H	Thermal conductivity (k)	$0.2 \frac{W}{m \cdot K}$
PROMATECT-H	Specific heat capacity (c_p)	$0.92 \frac{kJ}{kg \cdot K}$
PROMALITE-1200	Emissivity (ϵ)	0.95

The second and third heat transfer simulations were done using temperature-dependent material properties for PROMATECT-H and PROMATECT-L500. Since the temperature-dependent material properties of PROMATECT-H and PROMATECT-L500 were not available via the vendor, the bulk density, specific heat, and thermal conductivity measured by Steau and Mahendran [5] were used. Although Steau and Mahendran do not identify the calcium silicate boards by their Promat-designated names, they reference the Promat, Inc. website when identifying the commercial calcium silicate boards. Thus, the material properties given in [5] were used. Figure 3 shows temperature dependent a) density, b) thermal conductivity, and c) specific heat and mass loss for PROMATECT-H (left) and PROMATECT-L500 (right). Although a decomposition model was not included in this study, the decreasing bulk density of the decomposing calcium silicate boards was used (see Figure 3a). The thermal conductivity and specific heat of the decomposing calcium silicate boards was also used. Figure 3c shows that a decrease of approximately 25% mass occurs when PROMATECT-H reaches 200°C and PROMATECT-L500 reaches 800°C. Figure 3c was used to determine if mass loss should be expected when a hydrogen flame increases the temperature of these materials.

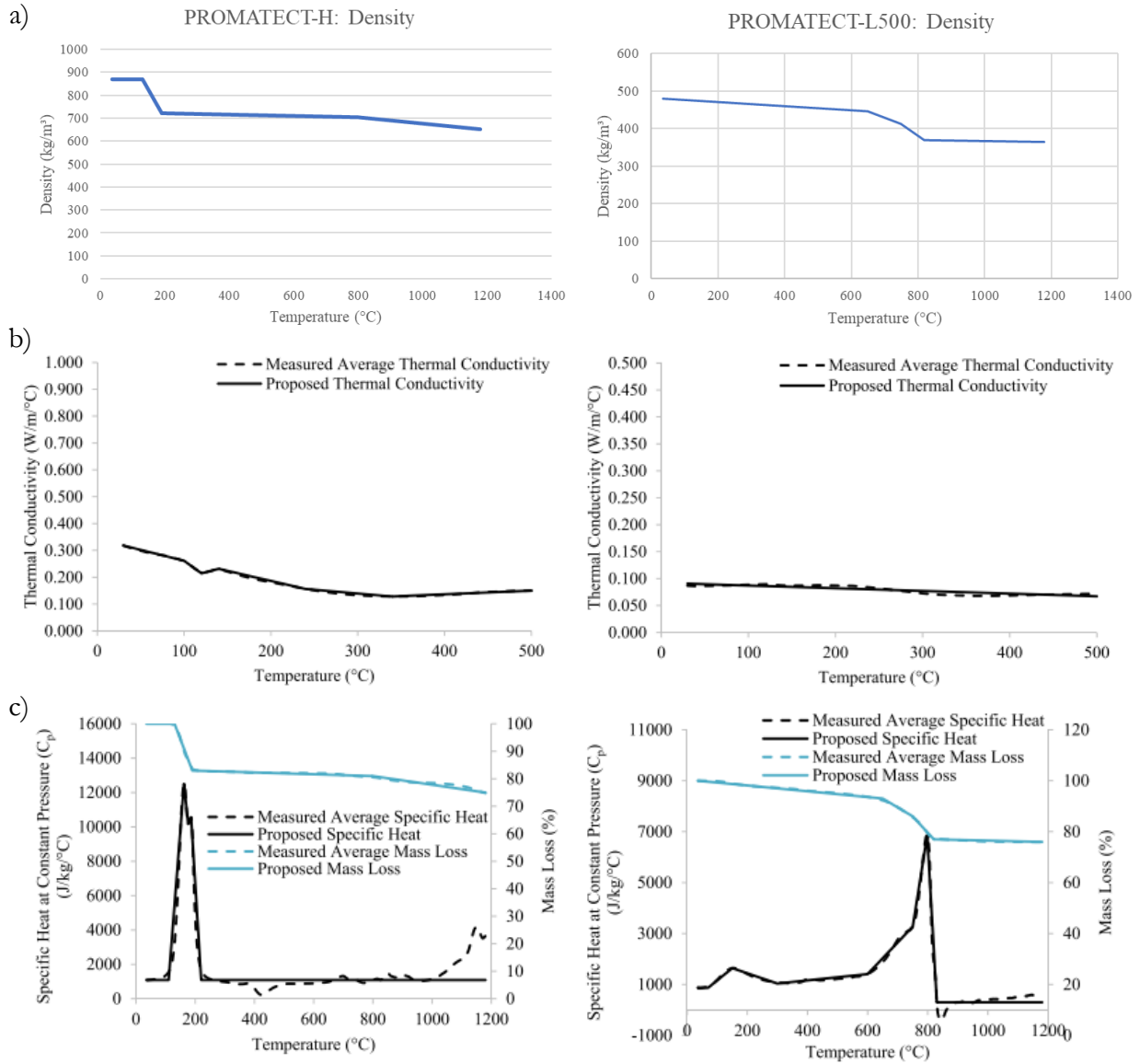


Figure 3. Temperature dependent a) density, b) thermal conductivity, and c) specific heat and mass loss for PROMATECT-H (left) and PROMATECT-L500 (right) [5].

2. NUMERICAL SIMULATIONS

A heat transfer analysis was performed to determine whether the heat from the hydrogen jet flame reaches the stainless-steel hangers and the epoxy anchoring the stainless-steel hanger to the tunnel surface. If the temperature reaches the degradation temperature of epoxy ($T_{e,d} = 90^{\circ}\text{C}$) at the anchors, then the epoxy starts degrading, and the hangers and fire protective board could collapse. The fire protective board was modeled as one 2-inch (5.08 cm) board, and the bounding material and porcelain enamel were ignored. The temperature at the location where the two 1-inch (2.54-cm) fire protective layers meet (1 inch (2.54 cm) from the surface) was highlighted; however, in this work, it was not possible to conclude whether the material used to bind together the layers could be compromised, since that material was identified. Since the fire protective slab acts as a barrier between the hydrogen jet flame and the hangers, only the fire protective slab was modeled to determine whether heat would penetrate the fire protective slab and reach the hangers. The hangers, the bolts, the washers, and the gap with the silicone were not included in the model. Though the tunnel also has exhaust vents every six fire protective boards, the scenario where the hydrogen jet flame impinges on the exhaust vents was not investigated. This study only considered the scenario where the hydrogen jet flame impinges on the fire protective board.

2.1. Numerical Domain

The Callahan tunnel numerical domain for simulations was a rectangular slab with a length of 600 inches (1524 cm) and a width of 280 inches (712.6 cm). The thickness of the slab, th , in Figure 4 was $th=2$ inch (5.08 cm). The temperatures at n -locations along the thickness of the slab (see Figure 4) are presented in Section 3. Starting at the center of the bottom surface ($x = z = y = 0$), the temperature at every $\Delta y = 0.2$ inch (0.5 cm) is represented as T_1, T_2, \dots , and $T_{n=11}$, as shown in Figure 4. T_1 is at $x = z = y = 0$, where the flame impinges, and T_n is at $x = z = 0$ and $y = th = 2$ inches (5.08 cm), where the hangers are attached to the fire protective board. T_6 is located where the two 1-inch Promat boards are bound together with the adhesive. Only the temperatures at $x=z=0$ along y were plotted to show how the temperature increases along the thickness of the slab. The temperatures at $x = z = 0$ along y are not necessarily the maximum temperature. However, the temperatures at $x = z = 0$ are relatively close to where the maximum temperatures are predicted to occur, so the plotted temperatures give the reader a good estimate of how high the temperatures are at any given time. The maximum temperature of the whole structure as a function of time is also specified in Section 3.

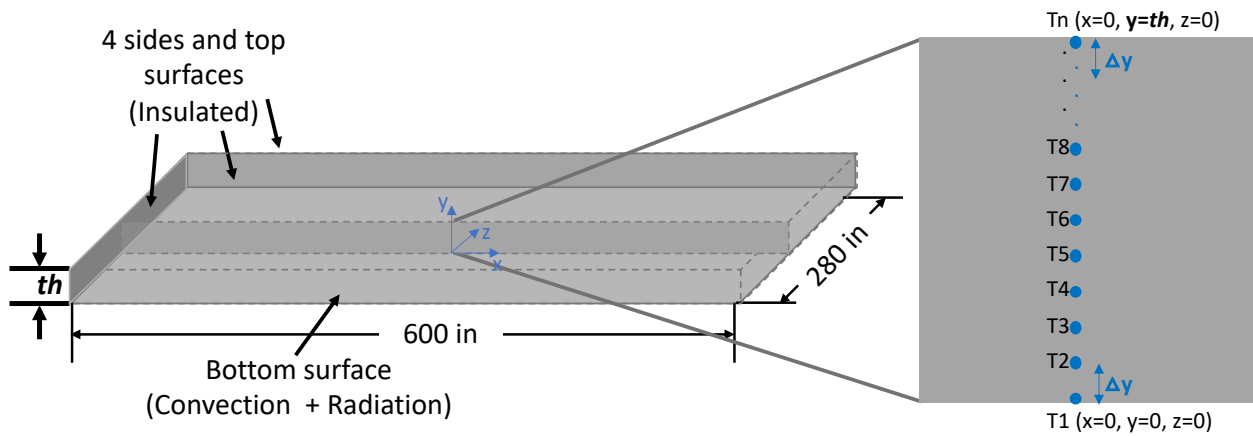


Figure 4: Isometric view of fire protective board used in heat transfer model. Fire protective board has a length of 600 inches (1524 cm), a width of 280 inches (713 cm), and a thickness of 2 inch (5.1 cm). All surfaces are assumed to be insulated except the bottom surface where convection and radiation are prescribed. Temperature T1-T11 are located every 0.2 inch (0.5 cm) across the thickness of the Promat. (Figure not to scale)

2.2. Mathematical Model

The Sierra module, Aria [3], was used to perform the heat transfer simulations. The model utilizes finite element method (FEM) to numerically solve the three-dimensional unsteady partial differential energy equation (PDE).

2.2.1. Energy Conservation Equation

To solve for the temperature, $T(x, y, z, t)$, as a function of time (t) and position (x, y, z) within the slab, the following PDE was derived from an energy balance where the heat conduction in the slab is equal to the sensible heat stored in the slab,

$$\rho c_p \frac{\partial T}{\partial t} - \nabla \cdot (k \nabla T) = 0 \quad \text{Equation 1}$$

where ρ is the bulk density, c_p is the specific heat, and k is the thermal conductivity of Promat for the Callahan tunnel. The Galerkin numerical method was used to discretize in space, and the finite difference method was used to discretize in time.

2.2.2. Initial and Boundary Conditions

The ceiling of the tunnel was assumed to have an initial ambient temperature, $T_{amb} = 25^\circ\text{C}$

$$T(t = 0) = T_{amb}. \quad \text{Equation 2}$$

As shown in Figure 4, the structure was assumed to be insulated on all surfaces except for the bottom surface, which encounters the hydrogen flame. In reality, the top surface will not be insulated since natural or forced (due to ventilation) convection and radiation losses will occur. However, assuming that the top is insulated defines a worst-case scenario. Convective and radiative heat transfer boundary conditions were applied at the bottom surface where the hydrogen jet flame impinges. The convective heat flux, \dot{q}_{conv}''' , applied to the surface is,

$$\dot{q}_{conv}''' = h(T_s - T_r) \quad \text{Equation 3}$$

where T_s is the slab surface temperature, h is the heat transfer coefficient, and T_r is the gas reference temperature. The radiative surface heat flux, $q_{n,r}$, is defined as the thermal energy emitted from the surface minus the incident energy,

$$q_{n,r} = \epsilon(\sigma T^4 - G) \quad \text{Equation 4}$$

where ϵ is the emissivity of the Promat, σ is the Stefan-Boltzmann constant, and G is the irradiation. Because the previously run CFD results for the no ventilation case showed that the hydrogen flame reaches a quasistatic state ~ 3.13 seconds into the simulation, the values for T_r , h , and G at 3.13 seconds (see Figure 5a) were used as the boundary conditions for the proceeding heat transfer analysis [4]. These values were assumed to remain constant in time for the 5 minutes needed for the hydrogen tank to empty in a real blowdown scenario. This is a conservative assumption; in reality, as the mass flow rate of the hydrogen exiting the TPRD decreases, the values for T_r , h , and G would also decrease. To facilitate the mapping of the CFD boundary conditions on this new tunnel structure, the values along the r -axis in Figure 5a were mapped to the slab surface. The center of the hydrogen flame ($r=0$ in Figure 5) was positioned at the center of the slab ($x=y=z=0$ in Figure 4). The temperature, heat transfer coefficient, and incident flux profiles were assumed to be circular contours with values shown in Figure 5b, c, and d.

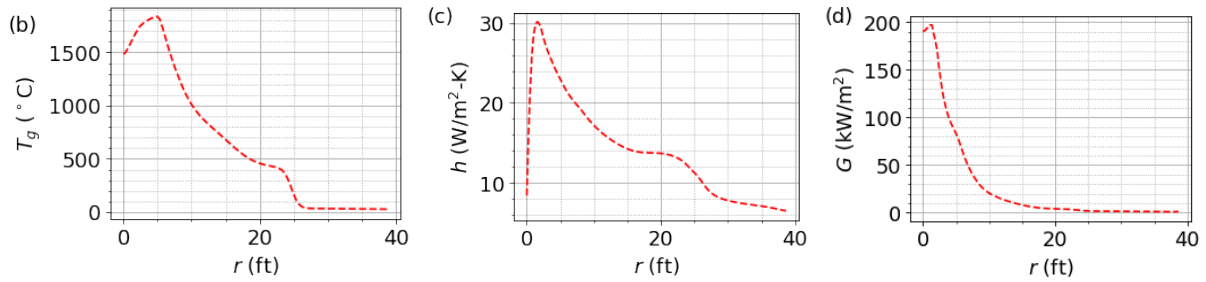
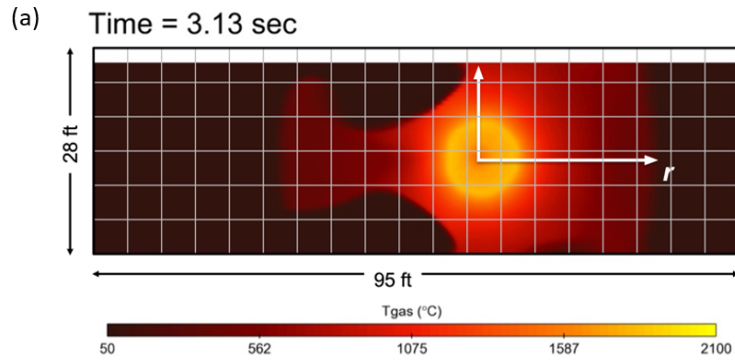


Figure 5. Boundary conditions applied on bottom surface of tunnel ceiling structure: (a) temperature map from [4], (b) the radial temperature, (c) convective heat transfer coefficient, and (d) irradiation plotted with respect to the r-axis measuring radial length from the center of the flame impingement on the bottom surface.

2.3. Mesh Refinement

A mesh refinement study was performed to ensure that the temperatures obtained across the slab are independent of the mesh size. A sufficiently fine mesh is required to accurately capture large temperature gradients. Since this heat transfer analysis primarily aims to observe how severely the heat penetrates the thickness of the slab, it is most important that the thickness of the slab be finely discretized more so than along its length or width. Thus, a mesh resolution study was performed until numerical results were independent of mesh resolution. Table 2 identifies the Promat type and the mesh used for each heat transfer simulation.

Table 2. Material properties and mesh used for each heat transfer analysis

Simulation	Promat Type	Material Properties	Mesh
1	PROMATECT-H	Constant	Fine
2	PROMATECT-H	Variable	Fine
3	PROMATECT-L500	Variable	Biased

2.3.1.1. Preliminary Refinement (Fine Mesh)

This study varied the number of intervals that span the thickness of the Promat slab to ensure that the results are independent of the mesh resolution. The interval size was refined until the temperature T_1 to T_{11} were independent of the mesh size. Figure 6 shows the temperature as a function of time at the bottom surface (top-left), and at 0.2 inch (top-right), 0.4 inch (bottom-left), and 0.6 in (bottom-right) from the bottom surface for intervals size of 2, 4, 8, 10, and 12. For an interval greater than or equal to 10, the mesh was sufficiently fine that the results were independent of the mesh resolution. Thus, the thickness was discretized into twelve intervals (as shown in Figure 7), and the resulting mesh

utilized for the heat transfer analysis contained 13,039,344 elements (14,155,050 nodes).

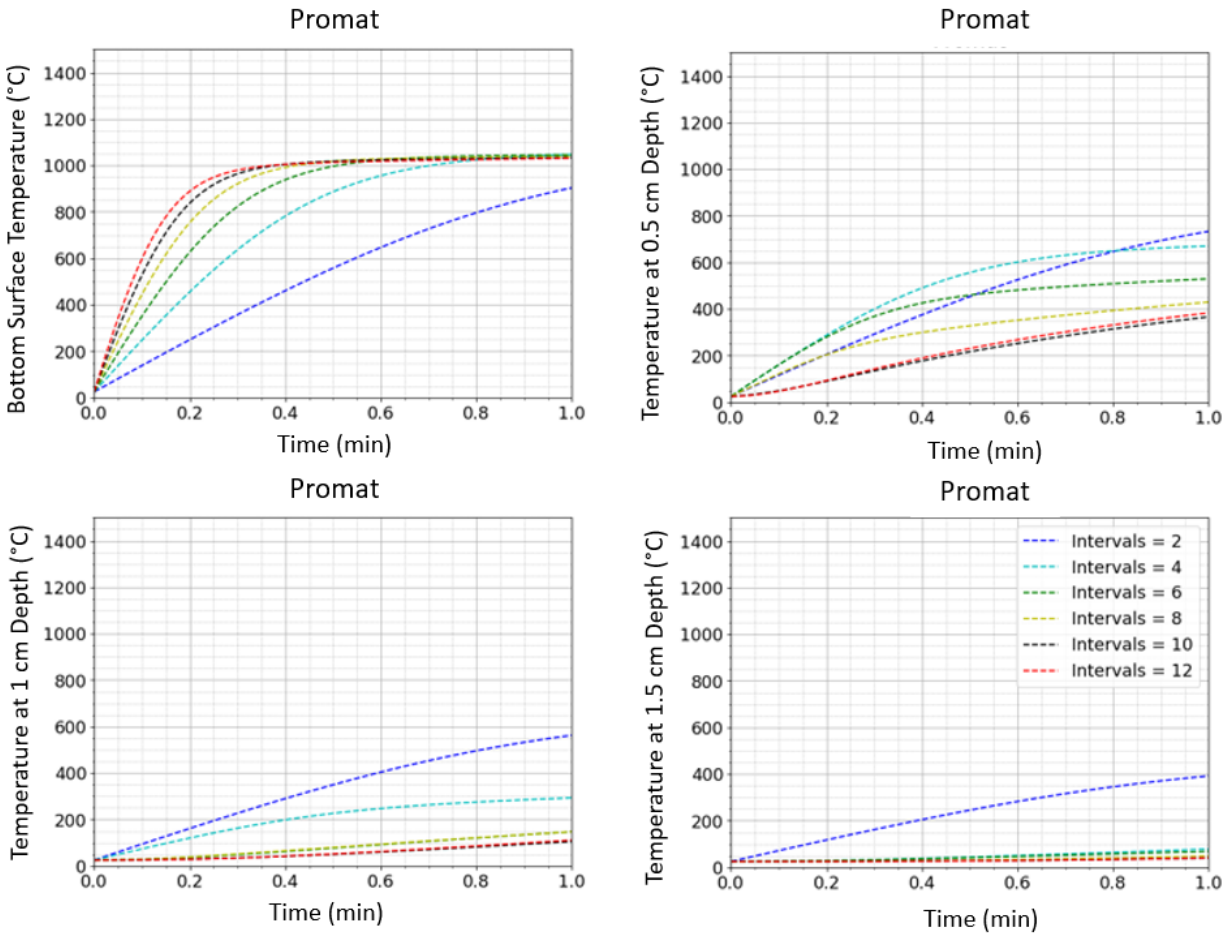


Figure 6. Temperature at the bottom surface (top-left), at 0.5 cm (top-right), 1.0 cm (bottom-left), and 1.5 cm (bottom-right) from the bottom surface for intervals 2 to 12. When the thickness is divided into 10 intervals or more, the mesh is sufficiently fine.

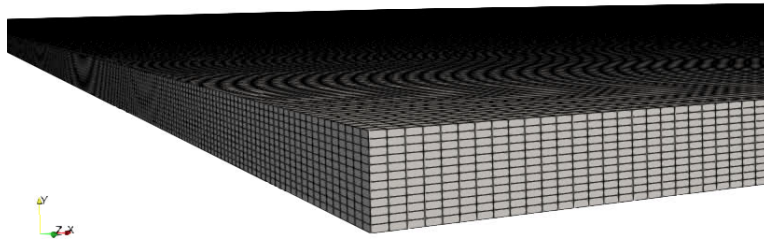


Figure 7. The final mesh used for the heat transfer analysis discretized the thickness of the Promat by 12 intervals. The mesh contains 13,039,344 elements (14,155,050 nodes).

2.3.1.2. Biased Mesh to Increase Efficiency

The mesh in Figure 7 is excessively large; the heat transfer simulation with that mesh had a run time of approximately 57 hours. Thus, further adjustment to the mesh was performed to decrease the computational expense. Since the goal was to obtain the maximum temperature in the structure, a coarse mesh was used far from the impingement area, and a finer mesh was used at the impingement area

where the highest temperatures are observed. From Figure 5a., the highest temperatures are on a radius of ~ 3.3 meters. Thus, the biased mesh shown in Figure 8 and Figure 9 is characterized by a circular profile of 3.3 meters in radial length. A bias mesh was created such that the center of the bottom surface has a finer grid spacing, and the mesh is progressively coarser going radially outward from the center of the circle. The element size at the edge of the radius of the circle was noted and enforced at the edges of the tunnel slab to preserve symmetry in the mesh.

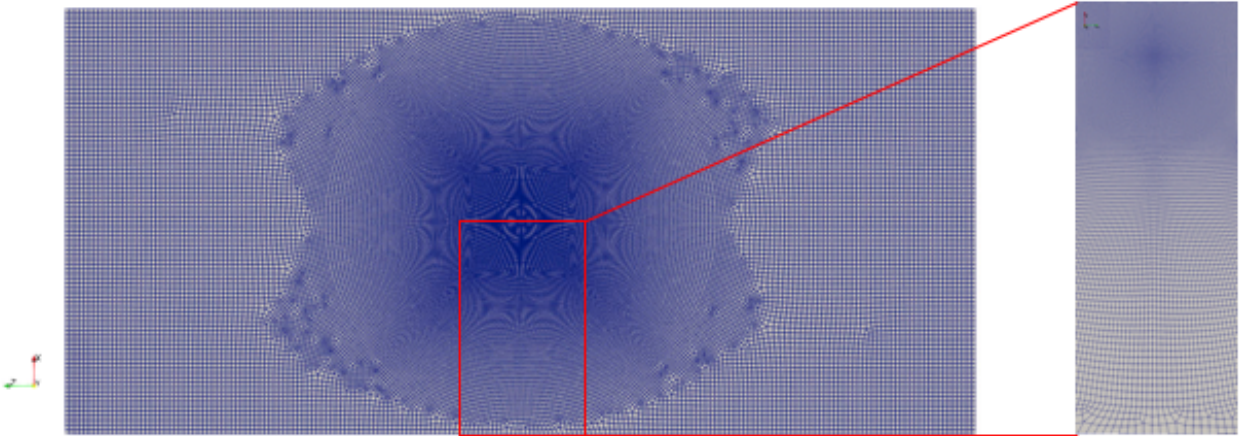


Figure 8. Bottom view of the biased mesh (left) and close-up bottom view of the biased mesh (right). A bias was applied within a 3.3 meters radius on the bottom surface. The element size on the outer radius was applied to the edges of the slab to preserve symmetry where possible.

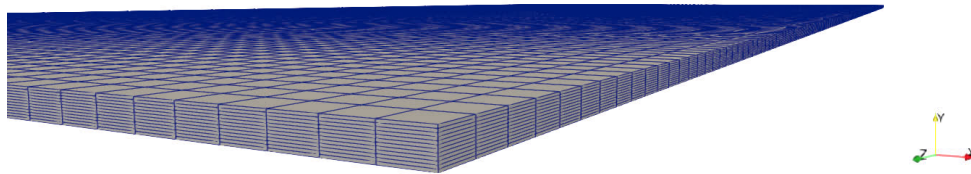


Figure 9. Isometric view of biased mesh used in Callahan tunnel simulations.

The heat transfer simulation for variable material properties of PROMATECT-H was run with the fine mesh and a biased mesh that concentrates the mesh nodes in the area where the temperature and heat flux is the highest and is coarser in the corners of the domain. These results were compared (Figure 10) to ensure that the accuracy produced by the fine mesh was sufficiently preserved. The bias mesh for the Callahan tunnel contains 549,528 elements (599,001 nodes) and provides a reduced run time of ~ 4 hours (compared to ~ 57 hours). Although the aspect ratio of the elements across the thickness of the slab is not optimal, simulation results were nearly identical to that of the fine mesh, so aspect ratio does not significantly compromise the results.

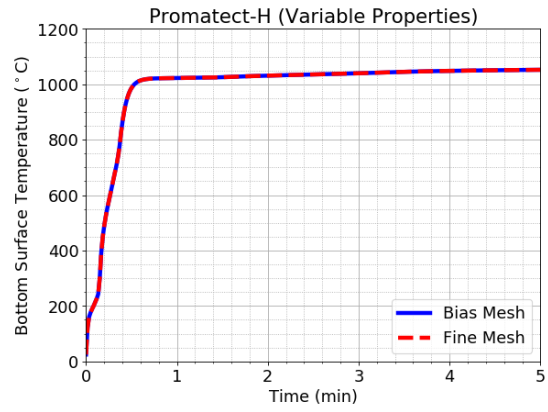


Figure 10. Heat transfer simulation results produced by the fine mesh and biased mesh were compared to ensure that the biased mesh produced sufficient accuracy. Plot shows the bottom surface temperature of PROMATECT-H over the span of 5 minutes.

3. RESULTS

This section presents the results for the Callahan tunnel. The temperature distributions on a cross-sectional view perpendicular to the z -plane at $z=0$ are displayed for time $t = 0$, 0.83 minutes, 1.3 minutes, and 5 minutes for each slab. The temperatures as a function of time at $x=z=0$ for different y -locations are also presented. A vertical dash-dotted blue line is positioned at 0.83 minutes to indicate when the 5 kg of hydrogen have been fully released at the mass flow rate used in the heat transfer simulations model. The other vertical dashed line at 1.3 minutes indicates when the flame is no longer impinging on the tunnel ceiling. Temperatures at $x=z=0$ are not necessarily the maximum temperature at a given y . Figure 5 shows that the maximum temperature of the flame is not at its center ($x=z=0$) but somewhere within 5 feet. It was not possible to find the maximum temperature at every given y , so instead only the temperatures at $x=z=0$ are plotted. For completeness, the maximum temperature in the whole structure is plotted with a red dashed line.

The temperature across the thickness for selected time steps are also included to show the specific location where the slabs are still at ambient temperature. In these plots, one can also find the depth at which possible decomposition may occur.

This section displays the temperature distributions for the 2-inch-thick Promat slabs—PROMATECT-H with constant material properties, PROMATECT-H with variable material properties, and PROMATECT-L500 with variable material properties.

None of the heat transfer simulations modeled the decomposition process that should happen at high temperatures. However, the density, thermal conductivity, and specific heat used in the heat transfer calculations were measured from an experiment where the materials were heated to high temperatures and decomposition of the material was achieved. An estimation of the mass loss, for both PROMATECT-H with variable material properties, and PROMATECT-L500 with variable material properties, was obtained by using the maximum temperature obtained from the simulations and finding the corresponding percentage of mass loss in Figure 3.

3.1. PROMATECT-H with Constant Material Properties

The first heat transfer simulation utilized the constant material properties for PROMATECT-H listed in Table 1. Using constant properties results in the highest temperature further inside the slab of the three cases investigated. Figure 11 shows the temperature distribution on a cross-section at $z=0$ for a 2-inch-thick Promat slab at time $t = 0$, 0.83 minutes, 1.3 minutes, and 5 minutes. A rapid increase in temperature at the bottom surface of the PROMATECT-H slab is observed. However, almost no temperature change is observed along the thickness of the slab. At 0.83 minutes, the maximum temperature at the bottom surface increases from ambient temperature (25°C) to 1064°C. The maximum temperature reaches 1064°C at 1.3 minutes. After 5 minutes, a more significant change can be observed along the thickness of the slab. However, even after 5 minutes, the top surface remains at ambient temperature of 25°C, which means the hangers are protected by the Promat slab.

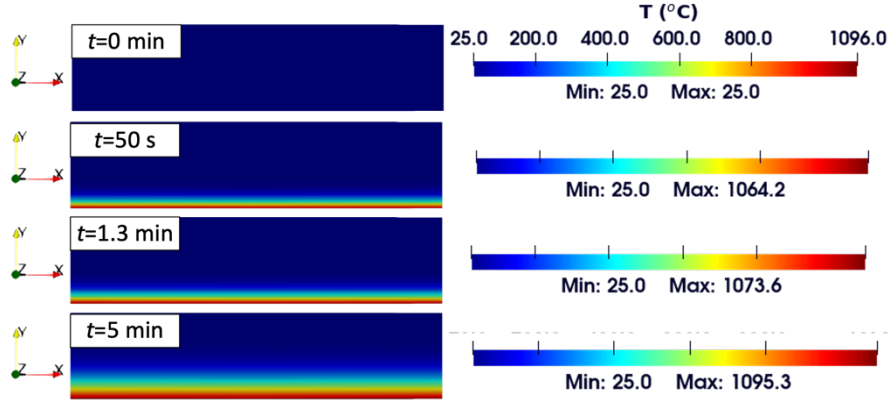


Figure 11. Temperature distribution across a 2-inch thick PROMATECT-L500 slab using variable material properties at different time steps. From top to bottom: 0, 0.83 minutes, 1.3 minutes, and 5 minutes. Maximum and minimum values are specified for each time step.

Figure 12a shows the maximum temperature of the structure (red dashed line) for a PROMATECT-H slab with constant properties, which is always going to be at the bottom surface ($y = 0$). The rapid increase in maximum temperature of the slab can be observed in Figure 12a. A maximum temperature of 1095°C is achieved in 40 seconds and remains constant after that. The temperatures at $x=z=0$ for different y -locations are also presented in Figure 12a and b. Figure 12b is a zoomed version of Figure 12a to show the temperatures at location 1-2 inches (2-5 cm) from the bottom surface. Note that the y -axis has a different scale to show how much the temperature increases at these locations.

At 0.83 minutes, the maximum temperature increases from ambient temperature to 1064°C. However, the temperature at 1 inch from the bottom surface is still ambient. At 1.3 minutes, the maximum temperature reaches 1073.5°C while the temperature at 1 inch from the surface is still ambient. After 5 minutes, the bottom surface reaches a temperature of 1095°C. At only 0.2 inch (0.5 cm) from the bottom surface, a significantly lower temperature (727.4°C) can be observed after 5 minutes. At 0.4 inch (1 cm) from the bottom surface, the temperature has only reached a value of 450°C after 5 minutes.

At 1 inch (2.5 cm), where the two board layers should be bonded together with an adhesive, the temperature only reaches 69.2°C after 5 minutes. Since the adhesive used to bond the two board layers is unknown, there is no way to know if the adhesive will degrade at 70°C. If this adhesive is similar to the epoxy used to anchor the hangers to the tunnel surface, then the adhesive should maintain a hold at 70°C since the degradation temperature is $T_{e,d} = 90^\circ\text{C}$. Figure 12(right) clearly shows that the temperature at the top surface where the hangers would be attached remains at ambient temperature.

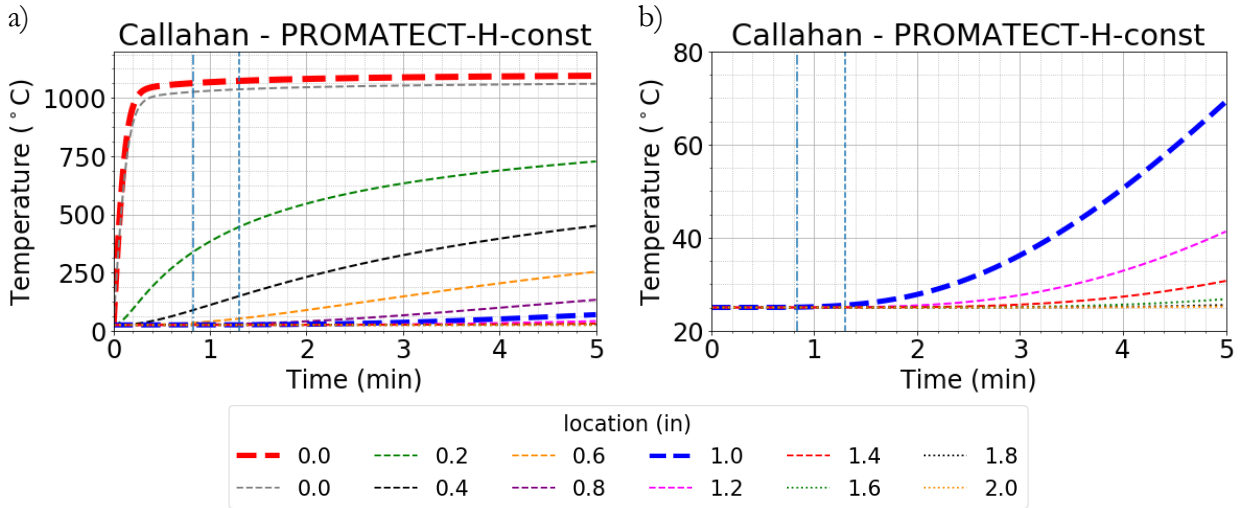


Figure 12. Transient temperature distributions at every 0.2 inch a) from the bottom surface ($y=0$) to the top surface ($y=2$ inches) and b) from $y=1$ inch to the top surface ($y=2$ inches) are shown for a PROMATECT-H slab with constant properties. Note that the scale of the y -axis on the figures is different.

3.2. PROMATECT-H with Variable Material Properties

The thermal properties measured by Steau and Mahendran were used for PROMATECT-H at temperatures ranging from 25°C to 1300°C. The results for temperature-dependent thermal properties are shown in Figure 13 and Figure 14. Compared to the simulation with constant material properties, Figure 13 shows a slower increase in temperature across the thickness of the PROMATECT-H slab. Again, the top of the PROMATECT-H slab remains undisturbed at a constant temperature of ~25°C.

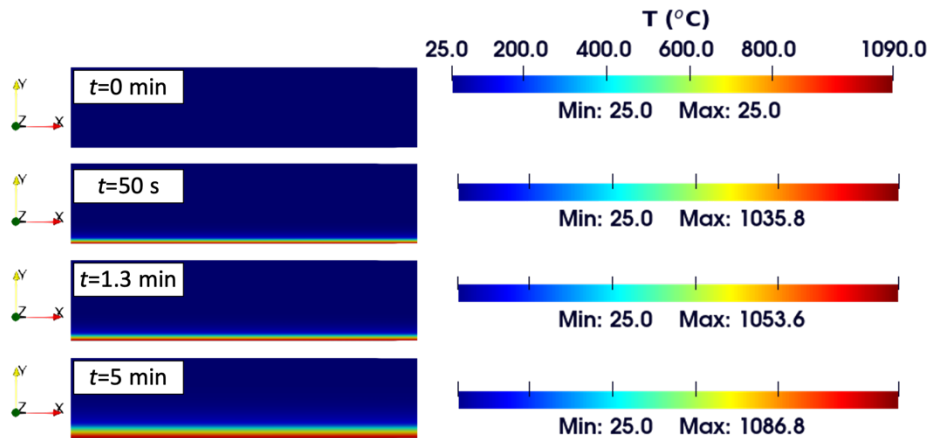


Figure 13. From top to bottom; temperature profile at center ($x=z=0$) of PROMATECT-H with variable material properties of thickness 2 inches (5 cm) at 0, 0.83 minutes, 1.3 minutes, and 5 minutes.

The simulation with variable properties predicts that slower heat conduction into the material than the simulations with constant properties. The simulations with variable properties show a slower temperature rise compared to the simulations with constant material properties. This can be explained by noticing that thermal conductivity decreases as temperature increases in Figure 3b(left). Figure 14a shows the maximum temperature of the structure (red dashed line) for a PROMATECT-H slab with

variable properties, which is always going to be at the bottom surface ($y = 0$). A maximum temperature of 1086.8°C is achieved in 1 minute and remains constant after that. Figure 14a also shows the transient temperature distributions at $x = z = 0$ for every $\Delta y = 0.2$ inch from the bottom surface ($y = 0$) to the top surface ($y=2$ inches). Figure 14b shows a zoomed version of a) to take a closer look at what the temperature are further away from the bottom surface. Note that the scale of the y -axis on Figure 14b is different than the scale on Figure 14a.

The temperature at the bottom surface takes more time to reach 1000°C compared to the simulations with constant properties. At 0.83 minutes, the maximum temperature increases from ambient temperature to 1035°C. However, the temperature at 1 inch from the bottom surface is still ambient. At 1.3 minutes, the maximum temperature reaches 1053°C and stays mostly constant after that. The temperature at 1 inch from the surface is still ambient at 1.3 minutes and reaches a maximum temperature of 39°C by 5 minutes.

The PROMATECT-H slab with variable properties experiences a temperature of 594.8°C after 5 minutes at 0.2 inch (0.5 cm) (versus 727.4°C for constant properties at same time and location). The maximum temperature at 1 inch from the bottom surface is 38.9°C, and at the top surface where the hangers are located, the temperature is still at 25°C. The results from the model with temperature dependent material properties will give more realistic results since thermal properties are in fact changing with temperature.

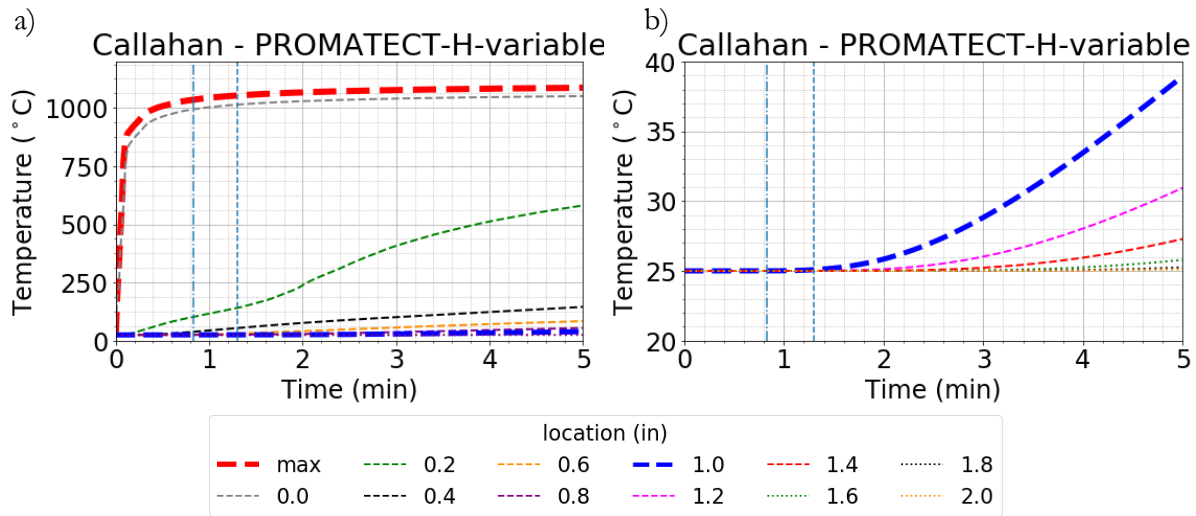


Figure 14. Temperature profile across the thickness for a Promat slab with variable properties of PROMATECT-H.

A 20-25% mass loss is expected at temperatures above approximately 150°C for PROMATECT-H (see Figure 3c-left). The depth for the decomposed material can be inferred from Figure 15. An average of 20-25% mass loss could happen up to $y = 0.4$ inch (1.5 cm) into the slab when a hydrogen jet flame impinges for 5 minutes. Figure 18 also clearly shows that where the two Promat slabs are bounded together with an adhesive ($y = 1$ inch (2.54 cm), marked with a dashed purple line), the temperature remains ambient.

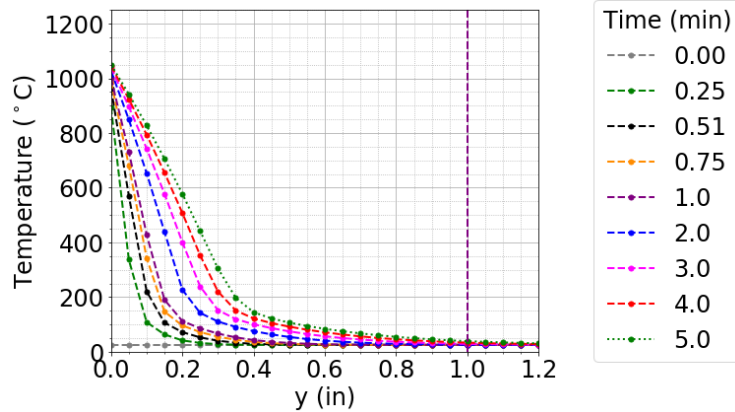


Figure 15. Temperature profiles across the thickness of the PROMATECT-H slab in the Callahan tunnel at different time steps show that at $y = 2$ inches the temperature is still ambient which corresponds to the location where the two slabs are attached.

3.3. PROMATECT-L500 with Variable Material Properties

The results of the heat transfer simulation with temperature dependent material properties for PROMATECT-L500 are presented in this section. Figure 16 show that the PROMATECT-L500 slab experiences a maximum temperature of 1106.7°C after 5 minutes, compared to 1086.8°C for PROMATECT-H with variable properties. The maximum temperature at 0.83 minutes and 1.3 seconds are 1088.4°C and 1094.6°C, respectively. At all times, the temperature at $y = 2$ inches remains constant at ambient temperature.

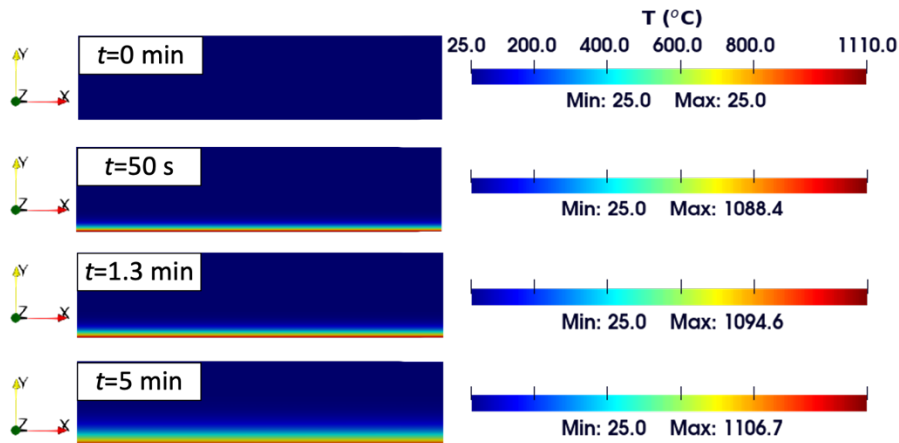


Figure 16. Temperature distribution across a 2-inch thick PROMATECT-L500 slab using variable material properties at different time steps. From top to bottom: 0, 0.83 minutes, 1.3 minutes, and 5 minutes. Maximum and minimum values are specified for each time step.

Figure 17a displays the maximum temperature of the PROMATECT-L500 and the temperature profiles at different location for PROMATECT-L500. A maximum temperature of 1106°C is achieved in 20 seconds and remains constant after that. This is significantly faster than the time PROMATECT-H takes to reach its maximum temperature. Figure 17b shows that the maximum temperature at 1 inch (2.54 cm) from the bottom surface only reaches 70°C. The top surface remains at 25°C after 5 minutes.

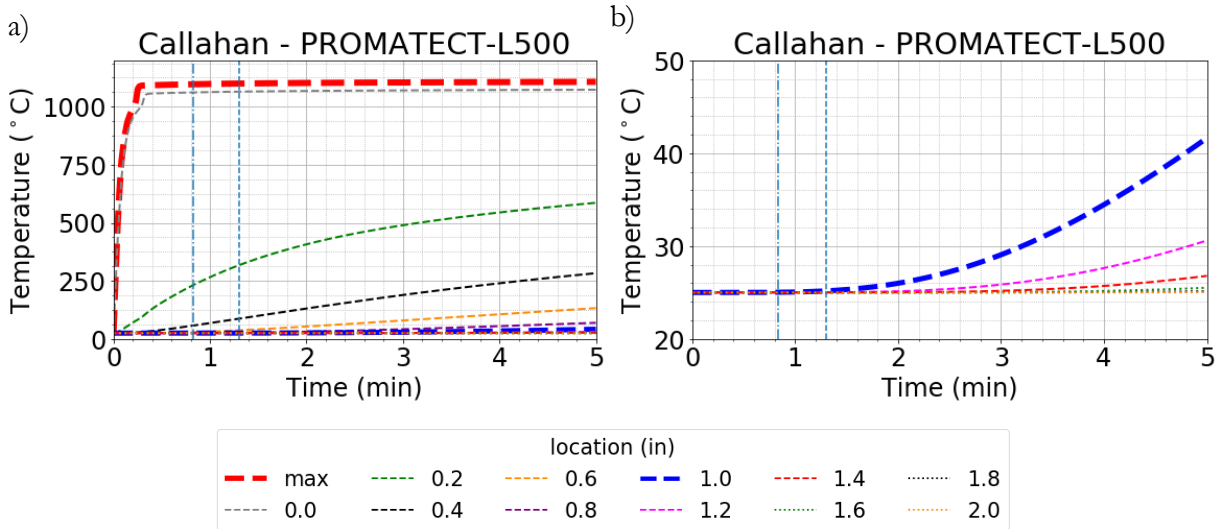


Figure 17. Temperature profile across the thickness for a Promat slab with variable properties of PROMATECT-L500.

The material will experience a 20-25% mass loss at locations where temperatures are above 600°C for PROMATECT-L500 according to Figure 3c-right. Figure 18 was used to determine that some mass loss should be expected between the bottom surface and 0.2 inch (0.5 cm) into the slab for a hydrogen jet flame impinging for 5 minutes. The location where the two Promat slabs are bounded together ($y = 1$ inch = 2.54 cm) is marked with a dashed purple line in Figure 18. The temperatures at $y = 1$ inch ($y = 2.54$ cm) and beyond remain at ambient temperature.

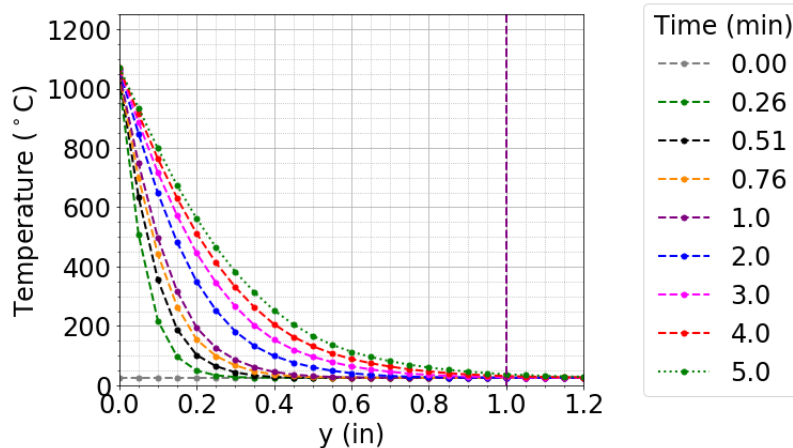


Figure 18. Temperature profiles across the thickness of the PROMATECT-L slab in the Callahan tunnel at different time steps show that at $y = 2$ inches the temperature is still ambient which corresponds to the location where the two slabs are attached.

3.4. Temperature at Adhesive Location

Figure 2 specifies two layers of 1-inch Promat material are adhered together (likely with PROMACOL-S). The location of 1 inch (2.5 cm) into the thickness of the Promat slab is of interest since this is where the adhesive is located. To evaluate what temperatures the adhesive experiences at the interface between the Promat layers, temperature was plotted with respect to time at this location ($x = z = 0$, $y = 1$ inch) for each of the heat transfer simulations (see Figure 19). PROMATECT-H (both constant and variable material properties) and PROMATECT-L500 do not reach temperatures above 70°C at this location. The PROMATECT-H slab reaches a maximum temperature of 69.2°C with constant properties and 41.4°C with variable properties. The PROMATECT-L500 slab reaches a maximum temperature of 41.6°C. If this adhesive is similar to the epoxy used to anchor the hangers to the tunnel surface, then the adhesive should maintain its integrity in this scenario since the degradation temperature of epoxy is $T_{ed} = 90^\circ\text{C}$.

The visible hydrogen jet flame is only expected to impinge on the ceiling for about 1.3 minutes. At this time, the PROMATECT-H slab with constant material properties experiences a temperature of 25.5°C at its center and halfway through its thickness (at 2.5 cm) where the adhesive is located. The PROMATECT-H slab with variable material properties and the PROMATECT-L500 slab experience temperatures of 25.3°C and 25.2°C, respectively, at this time and location.

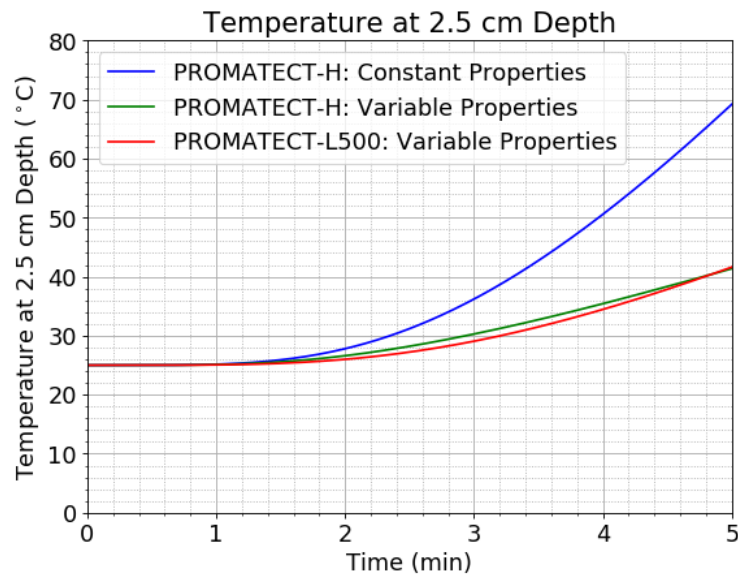


Figure 19. For each material, temperature profile with respect to time at the location of the adhesive which bonds two slabs of Promat

4. SUMMARY AND CONCLUSIONS

This report examined a scenario where a FCEV is overturned when it crashes with a gasoline vehicle. The TPRD is activated when gasoline from a leak ignites, creating an engulfing fire. The hydrogen released encounters heat from the fire, causing the hydrogen jet to ignite. When modeling assumptions were needed, conservative values were used so that the assumptions overestimate instead of underestimating the heat transfer to the tunnel. These assumptions were mainly applied to the convective and radiative heat transfer boundary conditions at the lower surface of the tunnel ceiling structure slab. The heat transfer coefficient, gas temperature, and incident heat flux obtained in the CFD simulations performed in [4] were used as boundary conditions in this study. The authors in [4] assumed a hydrogen release with constant mass flow rate for 5 minutes. This is a conservative assumption since the mass flow rate is expected to decrease with time resulting in a decrease in heat generation. In the CFD simulations, the amount of hydrogen that would be released in 5 minutes using a constant mass flow rate is 30 kg, not the 5 kg of a typical light-duty vehicle onboard storage tank. The 5 kg of hydrogen would be released in the first 0.83 minutes of those simulations. Results for a duration of 5 minutes were presented, but temperatures at 0.83 minutes and 1.3 minutes should be noted.

This work investigated the Callahan tunnel in Boston, Massachusetts for its test case. It was assumed that the hydrogen flame impinges on a passive fire protective board supported by stainless steel hangers anchored to the tunnel ceiling with epoxy. Only the fire protective board was modeled. Three cases with different properties for the protective board were run to determine if heat from the flame would reach the stainless-steel hangers and the epoxy causing the structure to collapse. Material properties from PROMATECT-H (constant and temperature dependent) and PROMATECT-L500 were used.

Table 3 summarizes important temperature values at 0.83 minutes, 1.3 minutes, and 5 minutes. Though the Promat slab is quite thin (2 inches or 5.08 cm) and conservative assumptions were employed, the numerical results show little deviation from ambient temperature at the top surface of the slab after 5 minutes for all three cases. This suggests that heat diffuses very slowly through the thickness of the Promat so that the top surface is nearly undisturbed by the heat conduction. Therefore, it was not necessary to perform additional analysis on the steel hangers since they are well protected by the Promat material. Promat provides adequate heat protection to the hangers during a hydrogen fire of five minutes duration.

Two layers of 1-inch (2.5 cm) Promat material are adhered together (likely with PROMACOL-S). The location of 1 inch (2.5 cm) into the thickness of the Promat slab is of interest since this is where the adhesive is located. The PROMATECT-H slab reaches a maximum temperature of 69.2°C with constant properties and 38.9°C with variable properties. The PROMATECT-L500 slab reaches a maximum temperature of 41.6°C. If this adhesive is similar to the epoxy used to anchor the hangers to the tunnel surface, then the adhesive should maintain integrity since the degradation temperature of epoxy is $T_{e,d} = 90^{\circ}\text{C}$. However, the degradation temperature of the adhesive used in this tunnel is unknown.

Promat will experience a 20-25% mass loss at locations where temperatures are above 150°C for PROMATECT-H and 600°C for PROMATECT-L500. For PROMATECT-H with constant properties, mass loss can be expected up to 1.0 cm from the bottom surface at 1.3 minutes and up to 1.5 cm at 5 minutes. For PROMATECT-H with varying properties, the damage will have penetrated 0.2 inch (0.5 cm) at 1.3 minutes and 0.4 inch (1 cm) at 5 minutes. For PROMATECT-L500, the

damage will have not penetrated past the bottom surface at 1.3 minutes. At 5 minutes, mass loss is expected up to 0.5 cm into the material. Although some damage is expected on the Promat material, authors estimate damage comparable to a longer (~60 minute) hydrocarbon fire.

According to these results, the passive fire protective board should provide adequate protection to the tunnel structure in the event of FCEV collision with a gasoline vehicle. Tunnel structures with similar suspended fire-resistant liner board materials should protect the integrity of the structure against the extremely low probability of an impinging hydrogen jet flame from a hydrogen TPRD release.

Table 3. Summary of temperatures of the Callahan tunnel at t = 0.83 minutes, 1.3 minutes, and 5 minutes.

Material	Properties	Time (minutes)	Temperature (°C)				
			Min. (y = 2 inches)	Max. (y = 0)	Bottom Surface (x = y = z = 0)	Center at y = 1 inch (x = z = 0)	Top Surface at y = 2 inches (x = z = 0)
PROMATECT-H	constant	0.83	25.0	1064.0	1026.6	25.1	25.0
		1.3	25.0	1073.5	1037.0	25.5	25.0
		5.0	25.0	1095.3	1060.9	69.2	25.0
	variable	0.83	25.0	1035.5	994.3	25.0	25.0
		1.3	25.0	1053.5	1014.37	25.08	25.0
		5.0	25.0	1086.8	1051.01	38.9	25.3
PROMATECT-L500	variable	0.83	25.0	1097.0	1061.9	25.02	25.0
		1.3	25.0	1100.0	1065.2	25.2	25.0
		5.0	25.0	1107.3	1073.3	41.6	25.0

REFERENCES

1. U.S. *National Clean Hydrogen Strategy and Roadmap*. 2023, U.S. Department of Energy.
2. *NFPA 502: Standard for Road Tunnels, Bridges, and Other Limited Access Highways*. 2023, National Fire Protection Association (NFPA).
3. *SIERRA Multimechanics Module: Aria User Manual-Version 4.56*. 2020, Sandia National Labs Report SAND-2021-3921: United States.
4. LaFleur, C.B., et al., *Hydrogen Fuel Cell Electric Vehicle Tunnel Safety Study*. 2017, Sandia National Laboratories Report SAND-2017-11157: United States.
5. Steau, E. and M. Mahendran, *Elevated temperature thermal properties of fire protective boards and insulation materials for light steel frame systems*. Journal of Building Engineering, 2021. **43**: p. 102571.
6. *Massachusetts Turnpike Authority Callahan-Summer Tunnels: Callahan Tunnel - Ceiling Replacement Cross Section II*. 1991, Howard, Needles, Tammen & Bergendoff (HNTB): United States.
7. *Massachusetts Turnpike Authority Callahan-Summer Tunnels: Callahan Tunnel - Ceiling Panel Details I*. 1991, Howard, Needles, Tammen & Bergendoff (HNTB): United States.
8. *Promat Boards for Tunnels*. 2023; Available from: https://www.promat.com/en-us/tunnels/products-systems/products/boards2/?page=1&page_size=18&sort=Id&sort_type=desc.
9. *Promat Technical Data Sheet. PROMATECT-H 2017 09/2017* [cited 2023 08/21/2023]; Available from: https://etex.azureedge.net/pd36273/original/-14737322/promatect-h_tds_en.pdf.
10. Singh, A., et al., *Design of a pilot scale directly irradiated, high temperature, and low pressure moving particle cavity chamber for metal oxide reduction*. Solar Energy, 2017. **157**: p. 365-376.

DISTRIBUTION

Email—Internal

Name	Org.	Sandia Email Address
Kristin Hertz	8367	klhertz@sandia.gov
Myra Blaylock	8751	mlblayl@sandia.gov
Gabriela Bran Anleu	8751	gabrana@sandia.gov
Camron Proctor	8751	cproct@sandia.gov
Brian Ehrhart	8854	bdehrha@sandia.gov
Chris LaFleur	8854	aclafle@sandia.gov
Technical Library	1911	sanddocs@sandia.gov

Email—External

Name	Company Email Address	Company Name
John Czach	john.czach@dot.state.ma.us	Massachusetts Department of Transportation
Christina Felipe	chtfelipe@gmail.com	FM Global
Haider Hamandi	haider.hamandi@dot.state.ma.us	Massachusetts Department of Transportation
Laura Hill	laura.hill@ee.doe.gov	DOE HFTO
Charles Myers	cmyers@massh2.org	Massachusetts Hydrogen Coalition, Inc.
Andrew Paul	andrew.paul@dot.state.ma.us	Massachusetts Department of Transportation
Joseph Rigney	rigney@delveunderground.com	Delve Underground

This page left blank



Sandia
National
Laboratories

Sandia National Laboratories is a multimission laboratory managed and operated by National Technology & Engineering Solutions of Sandia LLC, a wholly owned subsidiary of Honeywell International Inc. for the U.S. Department of Energy's National Nuclear Security Administration under contract DE-NA0003525.